The Impact of Reconstruction in Pandora on Sensitivity to the Low-Energy Excess Signal at MicroBooNE

The MicroBooNE Collaboration

MICROBOONE-NOTE-1114-PUB
microboone_info@fnal.gov

Abstract

With the MicroBooNE collaboration's first low-energy excess (LEE) searches complete and twice the amount of data to analyse in future iterations, it is imperative that we begin considering the potential analysis upgrades that can be achieved, such as those in the event reconstruction level. This note identifies the areas in Pandora reconstruction framework that could be improved upon, and evaluates their impact through cheated selections using MicroBooNE's exclusive pionless LEE search as a benchmark. Vertexing and proton reconstruction improvements are demonstrated to have significant potential benefits in terms of sensitivity to the LEE signal and thus should be prioritised. Sensitivity projections for the full $10.1e20$ POT are $3.2\,\sigma$ and $2.3\,\sigma$ for vertex and proton cheated selections respectively, and $3.3\,\sigma$ for the combined effect of both, compared to $2.1\,\sigma$ in the absence of the cheated selections.

Contents

1 Introduction

Anomalies in short-baseline appearance experiments hint at possible sources of new physics. An important example of this is the apparent low-energy excess (LEE) of ν_e events detected at accelerator neutrino experiments, such as LSND [1] and MicroBooNE's predecessor MiniBooNE [2]. Given the current understanding of neutrino oscillations in the 3-flavour framework, the appearance of ν_e in the beam is not expected at the baselines utilised by these experiments. One of MicroBooNE's primary physics goals is the characterisation of the LEE signal. This is facilitated by the use of a large LArTPC [3], which delivers unprecedented spatial and calorimetric resolution, allowing the experiment to probe neutrino interactions with complex multi-particle final states. The reconstruction of these intricate final state topologies is enabled through the Pandora Software Development Kit (SDK) [4][5]. It exploits a multi-algorithm approach to tackle specific topologies through the performance of small, manageable, pattern-recognition tasks, thus providing a framework to solve pattern-recognition problems in LArTPC environments.

The first round of results from MicroBooNE do not observe evidence of an excess [6][7]. There is twice the amount of data available that is yet to be analysed, hence now is the crucial time to begin considering potential upgrades in the analyses in order to be able to draw a conclusive picture about the nature of the excess in the future. In this article, areas for improvement at Pandora reconstruction level are identified (vertex finding and proton reconstruction) while keeping feasibility in mind. This is achieved through truth-based cheated selections on the existing Monte-Carlo (MC) data corresponding to 6.86e20 POT of the intrinsic ν_e component of the Booster Neutrino Beam (BNB). The cheated selections aim to demonstrate the impact of various aspects of reconstruction on the sensitivity to the LEE signal. The existing framework of the Pandora-based pionless LEE analysis [8], which probes two exclusive channels (with or without visible protons in the final state, called 1eNp and 1e0p respectively) is exploited and used as a benchmark.

2 Cheated Studies

Truth-based Vertex Cheated Selection (TVCS)

Figure 1 presents the vertex accuracy distributions (1eNp channel) at subsequent selection stages in the analysis. These show the distance between the reconstructed neutrino vertex and the true neutrino interaction point. Table 1 summarises the 90% quantiles of these distributions and efficiencies of each selection. It is prominent that vertex reconstruction failures are common. For example, at the early common preselection stage the 68% quantile is 9 cm, whereas the 90% quantile is 32.2 cm.

Selection Stage	**90% quantile [cm]**	**Efficiency**
Common preselection	[0.0-39.2]	100.0%
Np preselection	[0.0-39.3]	81.5%
Loose selection	[0.0-3.1]	29.3%
BDT selection	[0.0-2.0]	22.6%

Table 1: The range of (true - reconstructed) vertex distance containing 90% of the total events passing each selection stage. The common preselection efficiency is 100% because a slimmed down version of the ν_e sample used.

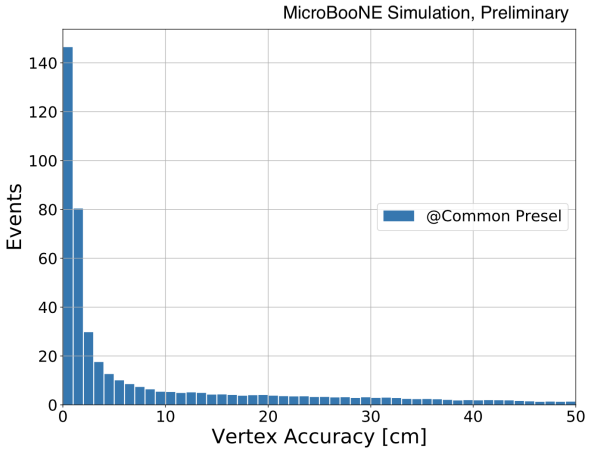

(a) Common preselection

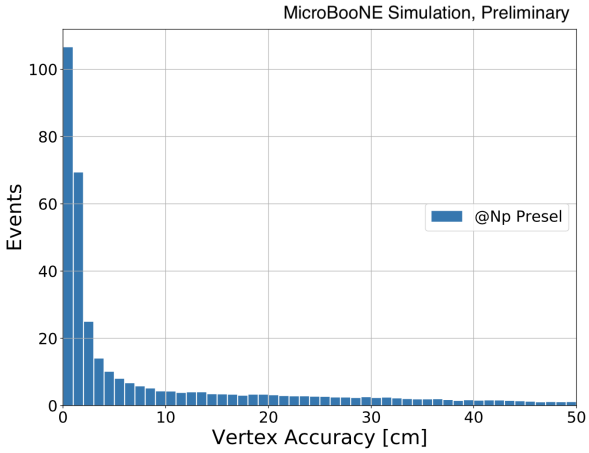

(b) 1eNp preselection

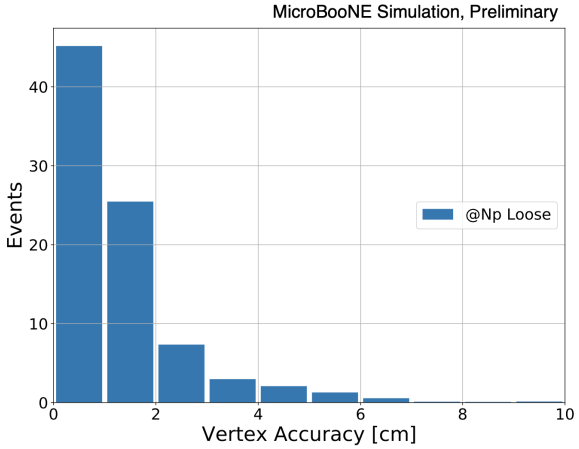

(c) Np loose selection

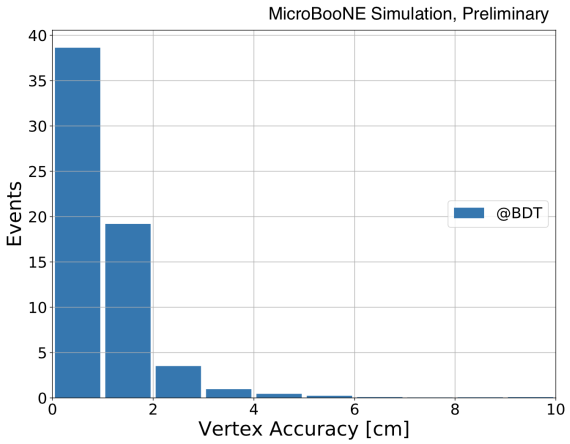

(d) NP BDT selection

Figure 1: Vertex finding accuracy at subsequent selection stages in the PeLEE analysis. At final two selection stages (1eNp Loose and BDT), the tail of distribution is short suggesting that the cuts applied are able to efficiently reject poorly-reconstructed events. This is not the case at the first two selections (common preselection and 1eNp preselection), which highlights the frequency of vertex reconstruction failures.

Table 2 outlines the cut-flow used in the TVCS. This cheated selection is different from vertex cheating that would usually be done within the Pandora framework, however the two should be correlated. Instead, it aims at determining whether improvements in vertexing could be impactful. Cuts in truth-space are applied to ensure containment and pionless final state signal topology with at least one or no protons for the 1eNp and 1e0p channels respectively. Subsequently, a vertex accuracy cut is applied to create a subset of original data sample and the events are fed through the established selections to evaluate their efficiencies (called *cheated efficiencies*, ϵ_{cheat}) for a given subset. These are presented in Figure 3 for the case when a vertex accuracy cut of 3 cm is used, together with ratios of baseline to cheated efficiency in true energy bins. For the

Variable	Comment
`isVtxInFiducial == 1`	Containment
`truthFiducial == 1`	
`npi0 == 0`	Correct signal topology
`npion == 0`	
`nproton == 0 / nproton > 0`	
`vtx_accuracy <= x`	Events with "well-reconstructed" vertex

Table 2: A summary of the cuts used for TVCS.

sensitivity estimation, the intrinsic ν_e component is re-scaled by the efficiency ratio (see Figure 2 for comparison of the intrinsic ν_e events before vs. after the scaling is applied). A scaling of 1-ϵ_{cheat} is applied to the backgrounds. To investigate the potential bias introduced by a hard vertex accuracy cut, the efficiency ratio is split up by interaction mode: quasi-elastic, resonant pion production, meson exchange current and deep-inelastic scattering. It is found that the percentage of events of each type and the ratio are consistent between the full sample and the subsample in these categories, indicating that meaningful conclusions may be drawn using this approach (see Appendix A.1).

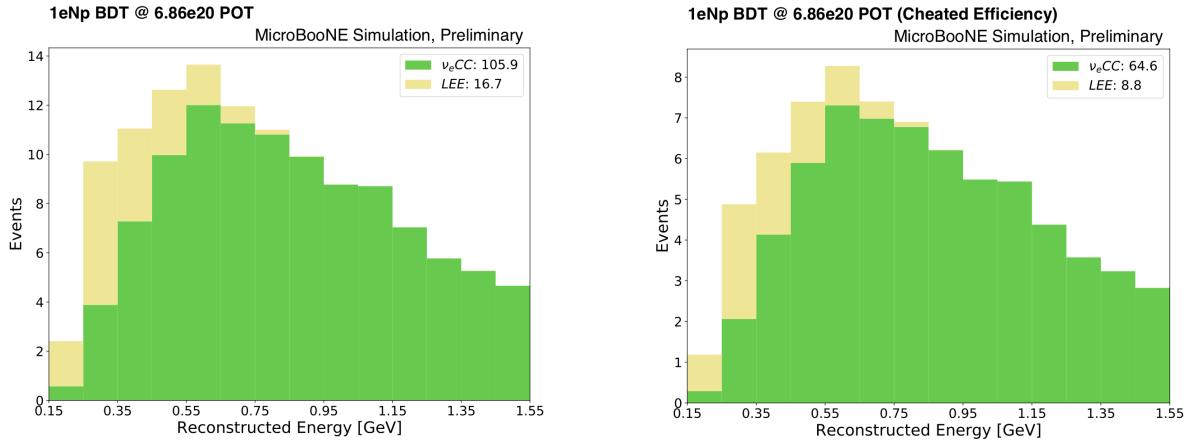

(a) (b)

Figure 2: Comparison of ν_e intrinsic events obtained for the 1eNp channel with (right) and without (left) the cheated efficiency weight. The rates of charged-current ν_e interactions and predicted LEE events increase by a factor of 1.67 and 1.90 respectively.

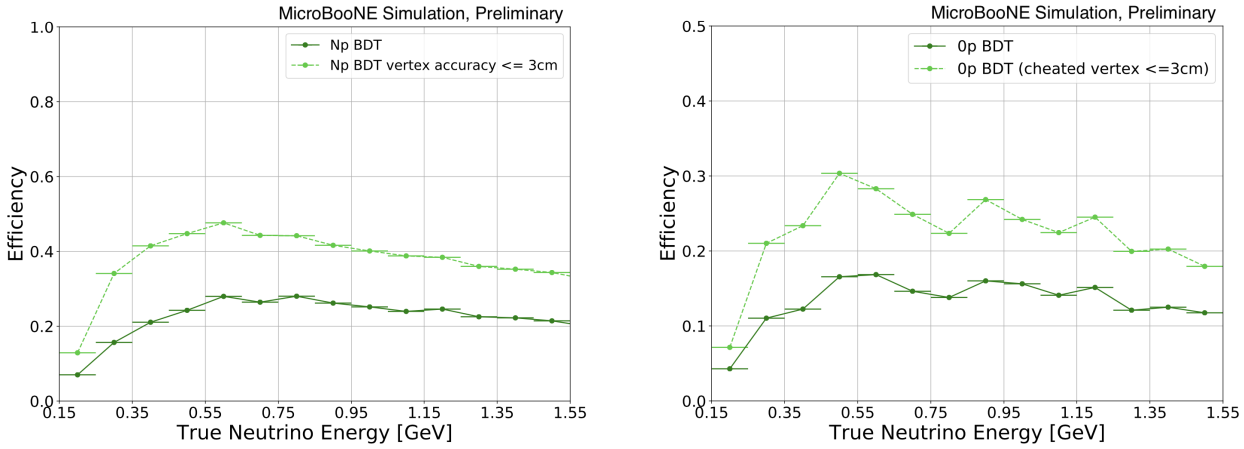

(a)

(b)

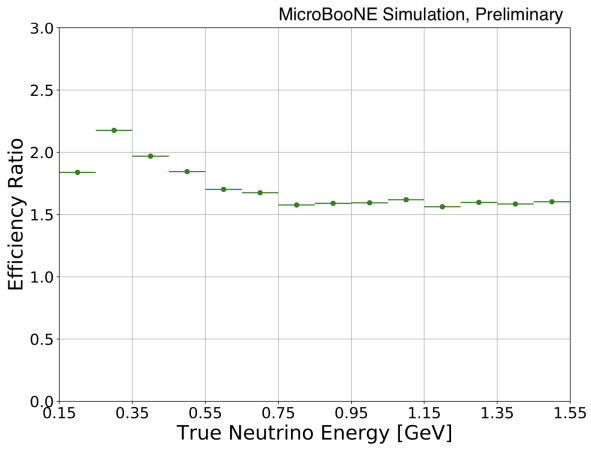

(c)

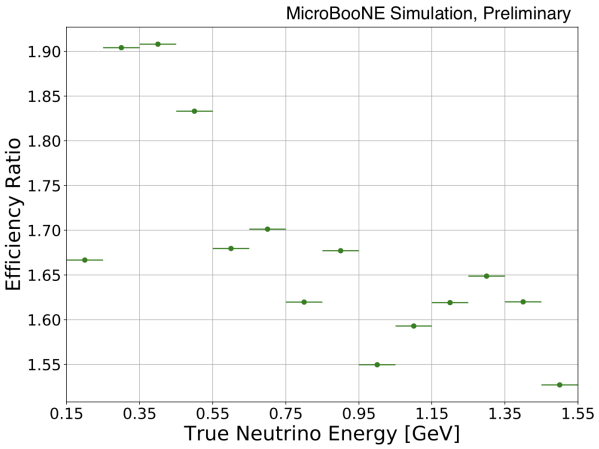

(d)

Figure 3: Top panel: Efficiency of (a) 1eNp BDT and (b) 1e0p BDT selections when applied to the ν_e intrinsic sample. The solid line shows the current efficiency and the dashed line represents the "cheated" efficiency obtained by restricting the selection cuts to a subset of the sample with a well-reconstructed vertex. Bottom panel: (c) 1eNp and (d) 1e0p efficiency ratio.

Truth-based Proton Cheated Selection (TPCS)

Table 3 outlines the cut-flow used in the TPCS. In similar manner to TVCS, truth-based cuts to ensure containment and correct signal topologies are applied. In addition to this, a true proton momentum threshold of $p = 300\,\text{MeV}$ is used. This corresponds to the minimum momentum for a proton track to likely be reconstructable in Pandora (see Fig 12 in Appendix A.2). A PID cut [9] is used to consider events with a proton-like track in the final state or events without a visible track. This selection is aimed at correcting for proton track reconstruction failures rather than track PID failures. Events which pass all these cuts constitute the reconstructable proton event sample (198.9 events). These are shown in Figure 4, which presents the number of reconstructed contained tracks vs. the number of true protons. Out of these, 17.5% events have no reconstructed proton tracks in the final state (corresponding to the bottom row of Figure 4). These are henceforth called the *missed proton events* and their contribution to the already selected intrinsic ν_e events, scaled by the baseline selection efficiency, is shown in Figure 5.

Variable	Comment
`isVtxInFiducial == 1`	Containment
`truthFiducial == 1`	
`npi0 == 0`	Correct signal topology
`npion == 0`	
`nproton >0`	
`proton_p >= 300 MeV`	Removing events with non-reconstructable proton tracks
`trkpid <0.02` or `trkpid > 9998`	Track identified as proton or event without visible tracks

Table 3: A summary of cuts used for TPCS.

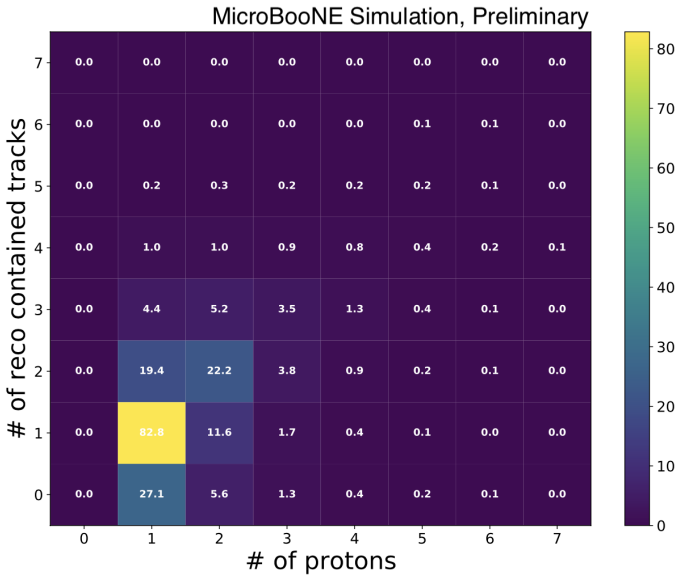

Figure 4: Proton multiplicity for neutrino events with reconstructable protons. The bottom row represents events which contained no reconstructed proton tracks in their final state.

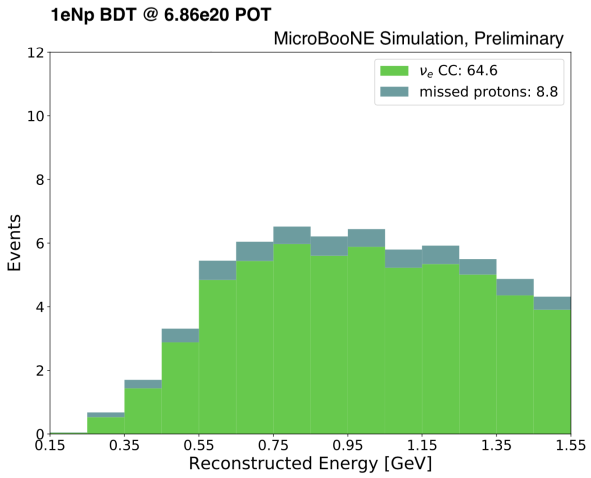

Figure 5: Missed protons events stacked on top of already selected events after accounting for selection efficiency.

Combining TVCS and TPCS

Vertexing and proton reconstruction are inherently linked within the Pandora framework (see Figure 6). To disentangle the combined effect of both, a vertex accuracy cut is included after applying the TPCS truth-cuts, but before the PID cut. In contrast to TPCS, the missed proton events selected in this manner are scaled by the cheated selection efficiency for a given vertex accuracy cut. This allows the investigation of the effect this additional contribution from missed proton events for a given definition of a well-reconstructed vertex has on sensitivity. The contribution for the case where a vertex accuracy cut of 3 cm is used is presented in Figure 7.

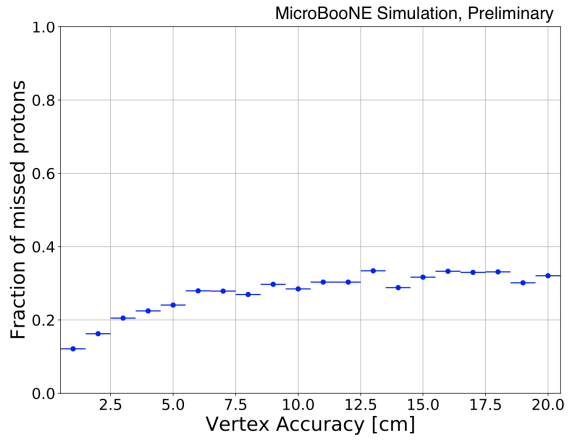

Figure 6: The 2D reconstruction of clusters, which correspond to track-like and shower-like objects, takes place prior to vertex finding during the Pandora neutrino pass. Once a vertex candidate has been identified, the algorithms which follow may alter the existing clusters in an attempt to boost the reconstruction efficiency based on the position of this vertex. Proton reconstruction failures are less frequent for events with a well-reconstructed vertex.

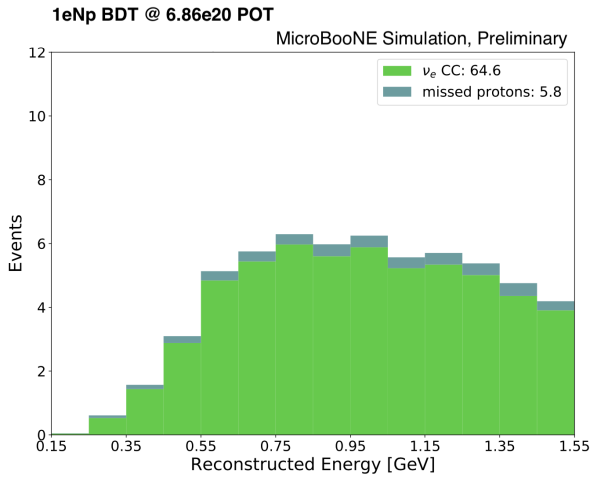

Figure 7: Missed protons events stacked on top of already selected events after accounting for the cheated selection efficiency.

3 Results

TVCS

Vertex cheated selections result in a significant improvement in efficiency across all energy bins, that is especially prominent in the low-energy region where the LEE is expected to occur (see Figure 3). Figure 2 shows how this leads to nearly doubling the statistics when the vertex accuracy cut off of 3 cm is used. Figure 8 presents the sensitivity results obtained via CNP formalism [10] using (a) the 3 cm cut and (b) varying the vertex accuracy cut. The sensitivity obtained via the cheated selection is $2.7\,\sigma$ (compared to the current $1.8\,\sigma$) for the vertex accuracy cut of 3 cm (see Figure 8(a)). When this cut is loosened to 9 cm the impact remains significant giving $2.4\,\sigma$ (see Figure 8(b)). This highlights the importance of vertex finding in neutrino event reconstruction and strongly emphasises the fact that improvements in the existing methods for vertexing in Pandora should be sought out.

TPCS

The number of selected missed proton events is shown in Figure 5. This overall contribution of 8.8 events is included in the sensitivity calculation, resulting is an increase in sensitivity from $1.8\,\sigma$ to $1.9\,\sigma$ (see Figure 9). While the impact of this cheated selection, which only considers the increase in selected events, is not as significant as the one obtained with TVCS, it is important to note that it does not probe other potential benefits of an upgrade in proton reconstruction, such as improved energy or proton multiplicity resolution. Both of these would be expected to further MicroBooNE's sensitivity to resolve the LEE signal.

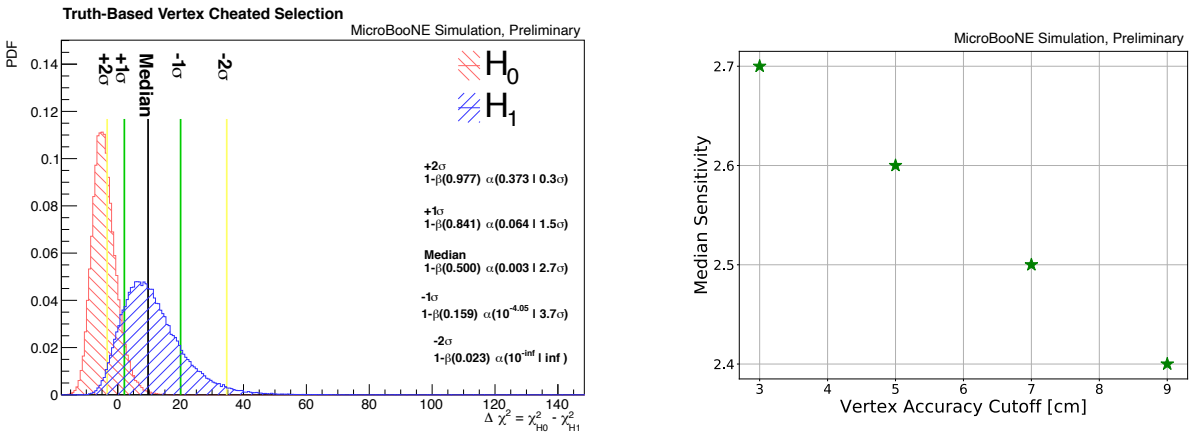

(a) (b)

Figure 8: (a) Sensitivity to reject the Standard Model as the null hypothesis (H_0) when TVCS is applied. 1-β and α represent the power of the test and the p-value of H_0 respectively. (b) Median sensitivity obtained with vertex cheating as the vertex accuracy cut is loosened.

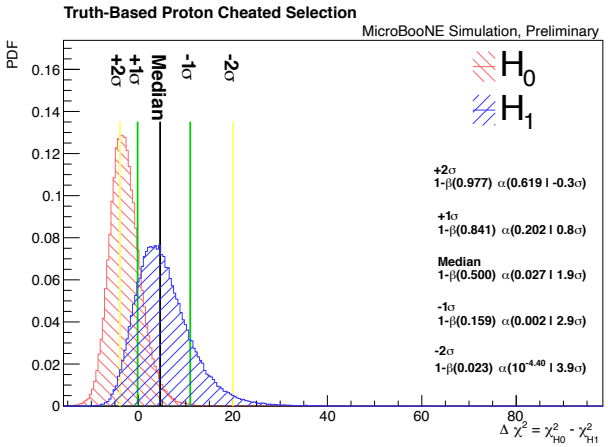

Figure 9: Sensitivity to reject the Standard Model as the null hypothesis (H_0), when TPCS is applied. 1-β and α represent the power of the test and the p-value of H_0 respectively.

Combined Contribution from TVCS and TPCS

For a vertex accuracy cut of 3 cm, the additional contribution from missed proton sample is 5.8 events after disentangling the effects of TVCS and TPCS. The sensitivity projection using this method is 2.8 σ (see Figure 10 (a)). Figure 10 (b) shows how the median sensitivity changes as the vertex accuracy cut is relaxed. At 9 cm the combined result from TVCS and TPCS is 2.6 σ (compared to 1.8 σ baseline and 2.4 σ for TVCS alone), which strongly suggest that proton reconstruction improvements should be pursued in parallel to vertexing upgrades.

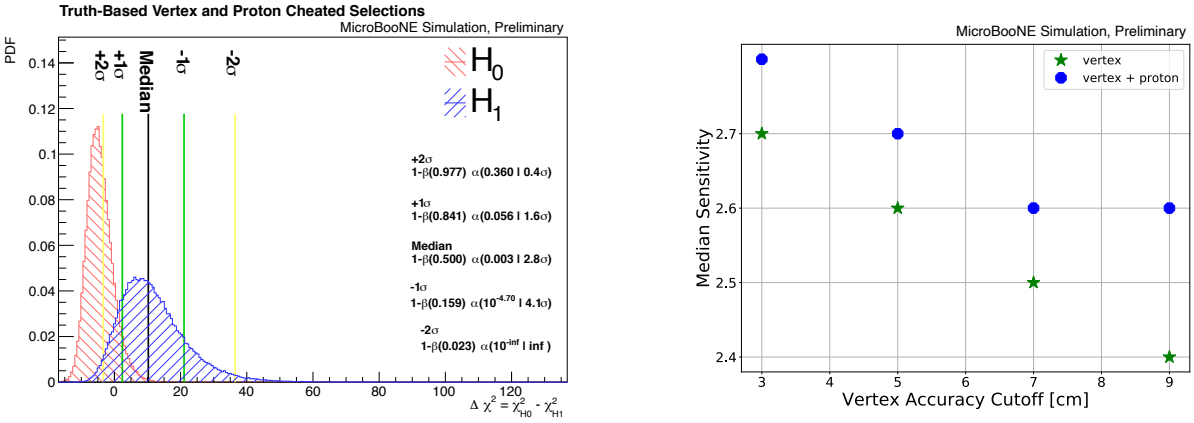

(a) (b)

Figure 10: (a) Sensitivity to reject the Standard Model as the null hypothesis (H_0), when TVCS and TPCS are combined. 1-β and α represent the power of the test and the p-value of H_0 respectively. (b) Median sensitivity obtained with proton cheating as the vertex accuracy cut is loosened.

Statistics Upgrade Sensitivity Projection

Table 4 summarises the results obtained with TVCS, TPCS and TVCS and TPCS combined. Sensitivities are shown at the benchmark point with vertex accuracy cut of 3 cm for the 6.86e20 POT (the POT of the unblinded data) and 10.1e20 POT (the POT of the full data sample available at MicroBooNE). The accompanying sensitivity plots are shown in Appendix A.3

	1e0p + 1eNp (6.86e20 POT)	**1e0p + 1eNp (10.1e20 POT)**
Current	1.8σ	2.1σ
Vertexing	2.7σ	3.2σ
Missed Protons	1.9σ	2.3σ
Combined	2.8σ	3.3σ

Table 4: Sensitivity projection using the cheated selections for the $6.86e20$ and $10.1e20$ POT samples.

4 Summary

This note summarises the investigation into the impact of improving vertex and proton reconstruction in Pandora using MicroBooNE's pionless LEE analysis as a benchmark. Two truth-based cheated selections are performed to deduce the additional contribution to the already selected intrinsic ν_e component of the beam that can be anticipated with a more more accurate vertex finding approach and when including the otherwise missed events with reconstructable protons in the final state. The impact of the cheated selections is quantified in terms of sensitivity. Vertex reconstruction is shown to be of key importance in terms of sensitivity to the LEE signal and should thus be prioritised. Furthermore, it is demonstrated that pursuing upgrades in proton reconstruction in parallel to vertexing would be beneficial in terms of fully utilising the available 10.1e20 POT neutrino beam data in the future.

A Appendix

A.1 Interaction Mode Dependence

Vertexing in Pandora is not random and its performance is affected by factors such as the complexity of the final state topology of the event. Thus, a potential bias may be introduced through the use of a hard vertex accuracy cut in the truth-based vertex cheated selection. To address this, the efficiency ratio computed at the benchmark point with a vertex accuracy of 3 cm for the intrinsic ν_e events is split up by different interaction modes: quasi-elastic (QE), resonant pion production (RES), meson exchange current (MEC) and deep-inelastic scattering (DIS). This is shown in Figure 11. The ratio remains constant in energy and is of similar magnitude (with the exception of the lowest energy region in which interactions proceed via QE). Most importantly, the fraction of events with a particular interaction mode is consistent between the full sample and the 3 cm subsample (within 0.1%). This suggests that events are scaled consistently across different interaction types, which in turn are correlated with the final state complexity, and the conclusions drawn from TVCS remain unchanged.

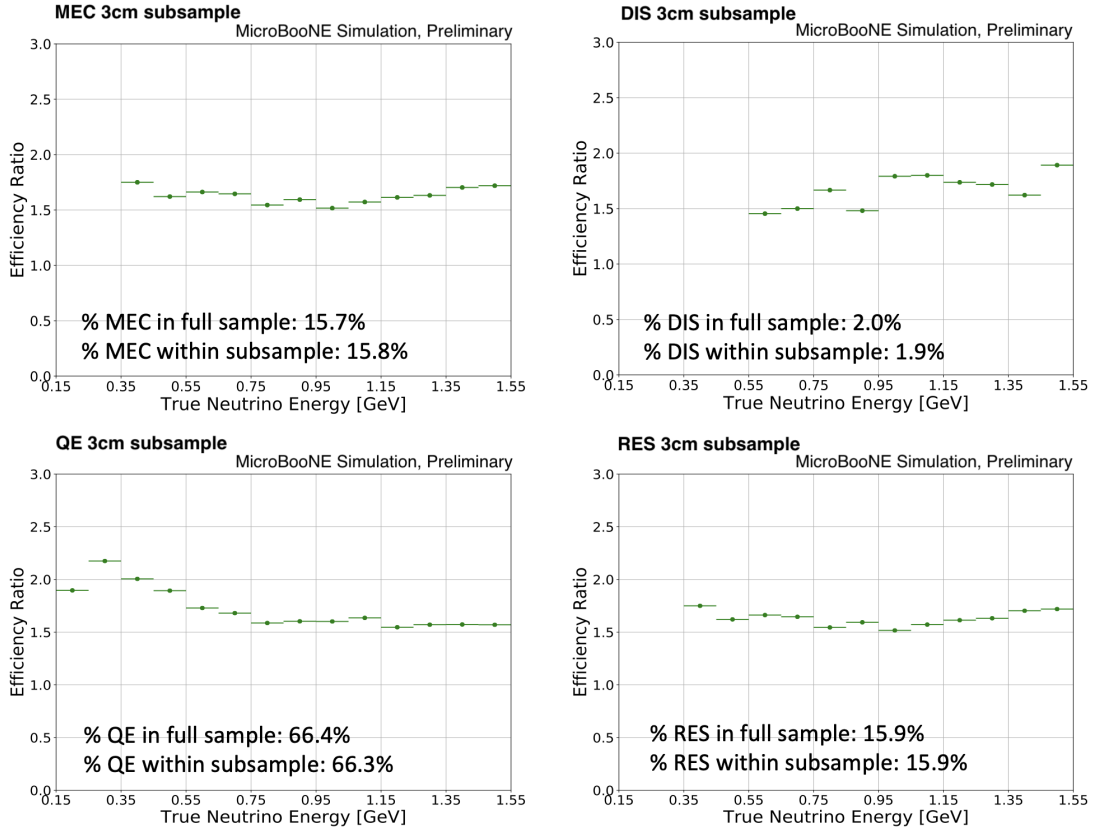

Figure 11: Efficiency ratio for the subsample of events with a vertex accuracy cut off at 3 cm split up by interaction type. The percentage of events which proceed via a particular interaction mode remains consistent between the full sample and the subsample.

A.2 Momentum Distribution of Protons in Pandora

Pandora reconstruction metrics require a certain number of hits to be present when evaluating performance (see Figure 12). This corresponds to 15 hits in total, including at least 5 hits in two of the three planes [4], translating to about 47 MeV of proton kinetic energy and a path length of 1.5 cm in liquid argon [11]. It becomes increasingly difficult to match hits between read-out planes when a low number of hits is present. Hence low momentum protons become less likely to be reconstructed efficiently and they can be missed.

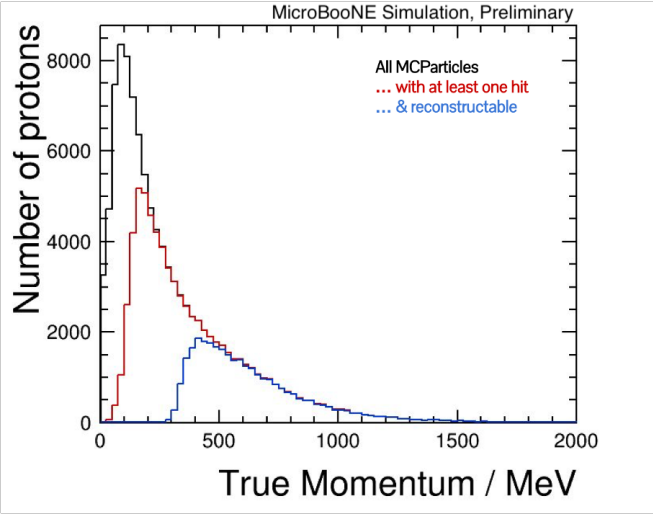

Figure 12: Proton true momentum distribution. The number of reconstructable protons (blue) is significantly smaller than that of the whole simulated sample (black).

A.3 Statistics Upgrade Sensitivity Plots

A.3.1 Statistics + TVCS

Full statistics (10.1e20 POT) upgrade sensitivity with TVCS (described in Section 2).

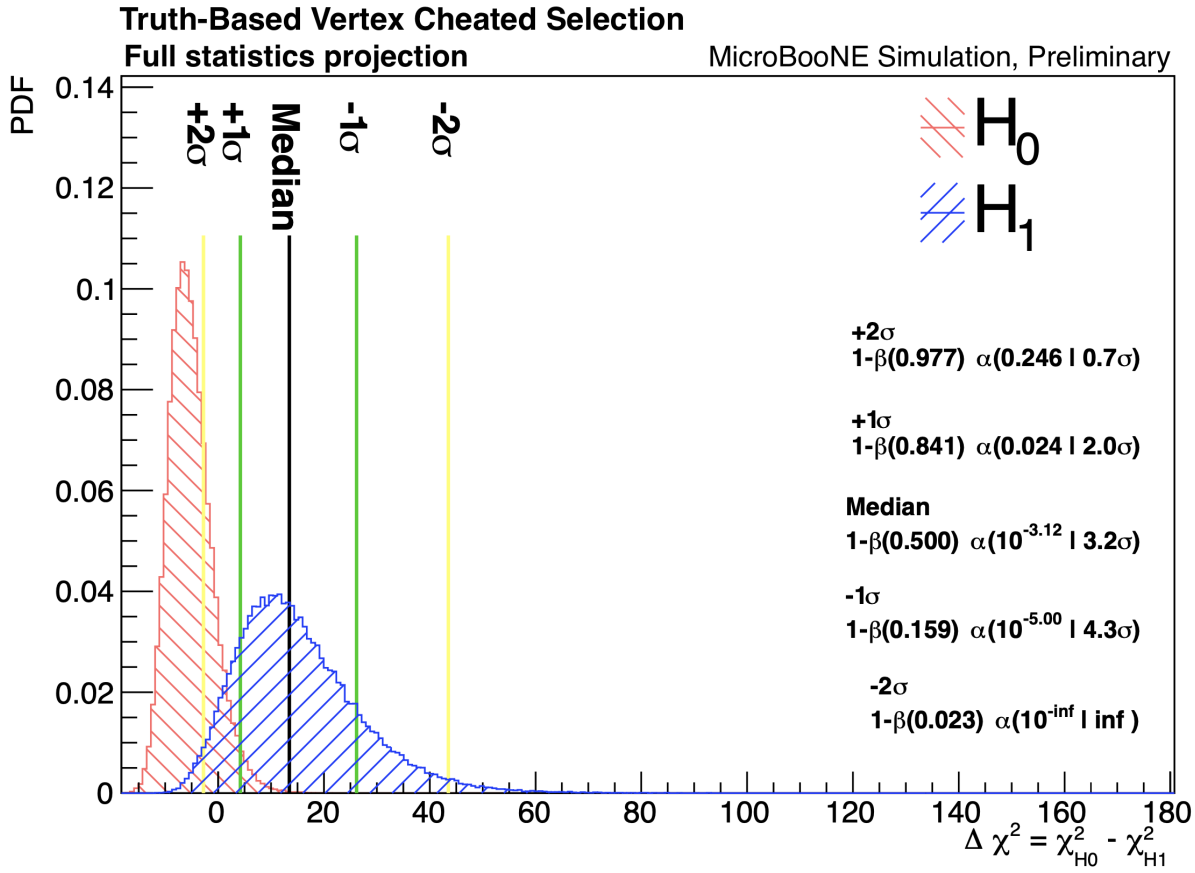

Figure 13: Full statistics sensitivity to reject the Standard Model as the null hypothesis (H_0), with TVCS. 1-β and α represent the power of the test and the p-value of H_0 respectively.

A.3.2 Statistics + TPCS

Full statistics (10.1e20 POT) upgrade sensitivity with TPCS (described in Section 2).

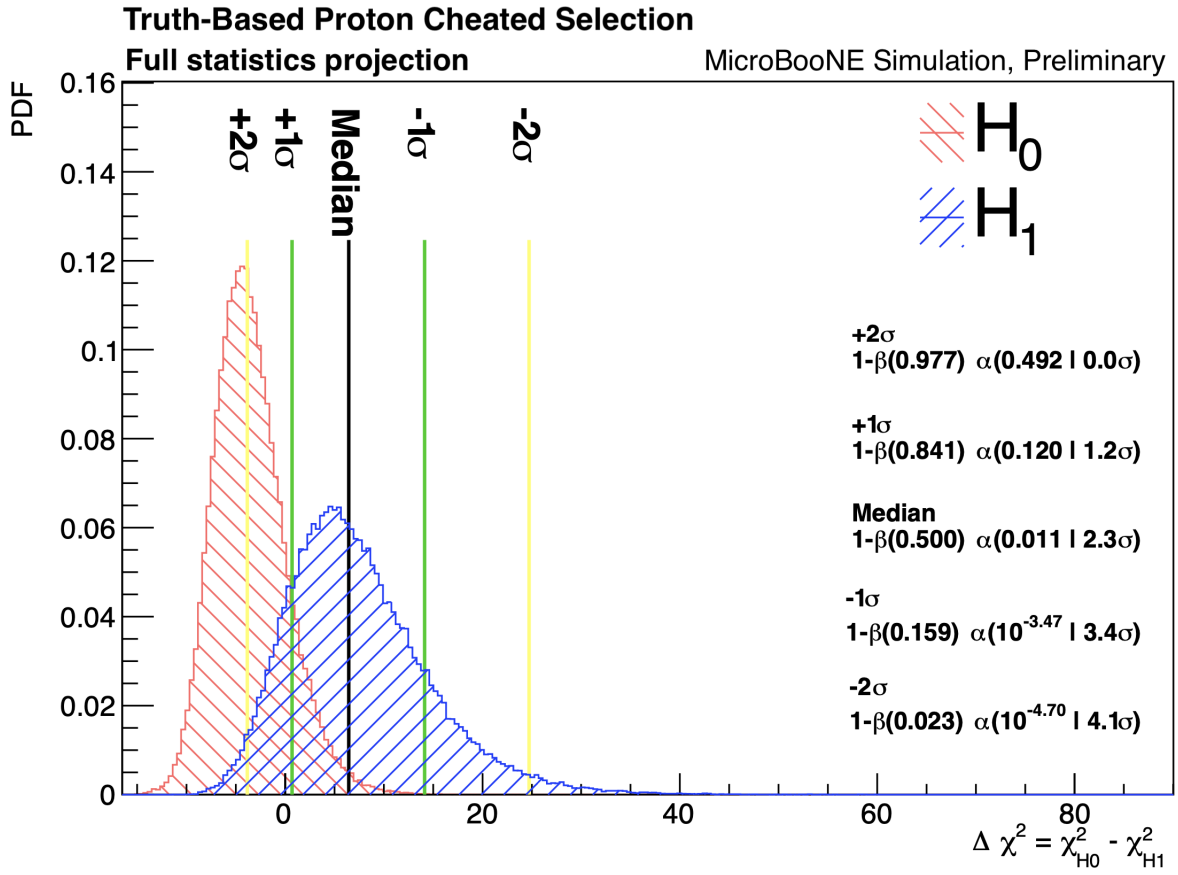

Figure 14: Full statistics sensitivity to reject the Standard Model as the null hypothesis (H_0), when TPCS is applied. 1-β and α represent the power of the test and the p-value of H_0 respectively.

A.3.3 Statistics + TVCS and TPCS Combined

Full statistics (10.1e20 POT) upgrade sensitivity with TVCS and TPCS combined (described in Section 2).

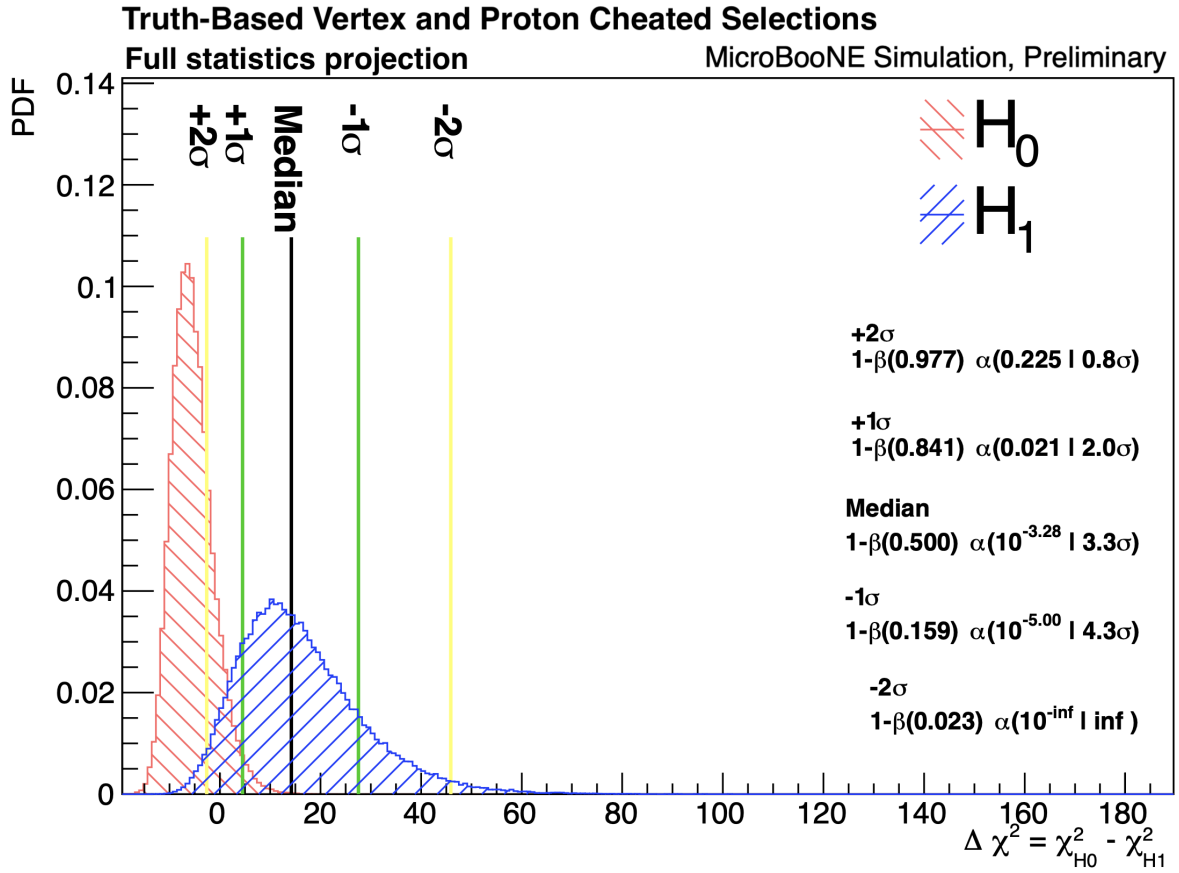

Figure 15: Full statistics sensitivity to reject the Standard Model as the null hypothesis (H_0), when TVCS and TPCS are combined. 1-β and α represent the power of the test and the p-value of H_0 respectively.

References

[1] The LSND Collaboration. *Evidence for neutrino oscillations from the observation of electron anti-neutrino appearance in a muon anti-neutrino beam*. Phys. Rev. D 64 112007. 2001. DOI: 10.1103/physrevd.64.112007.

[2] The MiniBooNE Collaboration. *Significant Excess of Electronlike Events in the MiniBooNE Short-Baseline Neutrino Experiment*. Phys. Rev. Lett. 121 221801. 2018. DOI: 10.1103/physrevlett.121.221801.

[3] The MicroBooNE Collaboration. *Design and construction of the MicroBooNE detector*. Journal of Instrumentation 12 P02017. 2017. DOI: 10.1088/1748-0221/12/02/p02017.

[4] The MicroBooNE Collaboration. *The Pandora multi-algorithm approach to automated pattern recognition of cosmic-ray muon and neutrino events in the MicroBooNE detector*. arXiv: 1708.03135.

[5] J. S. Marshall and M. A. Thomson. *The Pandora software development kit for pattern recognition*. Eur. Phys. J. C 75 439. 2015. DOI: 10.1140/epjc/s10052-015-3659-3.

[6] The MicroBooNE Collaboration. *Search for an Excess of Electron Neutrino Interactions in MicroBooNE Using Multiple Final State Topologies*. 2021. arXiv: 2110.14054.

[7] The MicroBooNE Collaboration. *Search for Neutrino-Induced Neutral Current Radiative Decay in MicroBooNE and a First Test of the MiniBooNE Low Energy Excess Under a Single-Photon Hypothesis*. Phys. Rev. Lett. (accepted for publication). arXiv: 2110.00409.

[8] The MicroBooNE Collaboration. *Search for an anomalous excess of charged-current ν_e interactions without pions in the final state with the MicroBooNE experiment*. Phys. Rev. D (accepted for publication). arXiv: 2110.14065.

[9] The MicroBooNE Collaboration. *Calorimetric classification of track-like signatures in liquid argon TPCs using MicroBooNE data*. J. High Energ. Phys. 2021 153. 2021. DOI: 10.1007/jhep12(2021)153.

[10] J. Xiangpan et al. *Combined Neyman–Pearson chi-square: An improved approximation to the Poisson-likelihood chi-square*. Nuclear Instruments and Methods in Physics Research Section A: Accelerators, Spectrometers, Detectors and Associated Equipment 961 163677. 2020. DOI: 10.1016/j.nima.2020.163677.

[11] The MicroBooNE Collaboration. *Measurement of differential cross sections for ν_μ-Ar charged-current interactions with protons and no pions in the final state with the MicroBooNE detector*. Phys. Rev. D 102 112013. 2020. DOI: 10.1103/PhysRevD.102.112013.